ELSEVIER

NeuroImage

www.elsevier.com/locate/ynimg
NeuroImage 33 (2006) 46 – 54

Increased local gyrification mapped in Williams syndrome

Christian Gaser,[a] Eileen Luders,[b] Paul M. Thompson,[b] Agatha D. Lee,[b] Rebecca A. Dutton,[b] Jennifer A. Geaga,[b] Kiralee M. Hayashi,[b] Ursula Bellugi,[c] Albert M. Galaburda,[d] Julie R. Korenberg,[e] Debra L. Mills,[f] Arthur W. Toga,[b] and Allan L. Reiss[g,*]

[a]*Department of Psychiatry, University of Jena, Jena, Germany*
[b]*Laboratory of Neuro Imaging, Department of Neurology, UCLA School of Medicine, Los Angeles, CA 90095, USA*
[c]*Laboratory for Cognitive Neuroscience, Salk Institute, La Jolla, CA 92037, USA*
[d]*Department of Neurology, Harvard Medical School and Beth Israel Deaconess Medical, Center, Boston, MA 02115, USA*
[e]*Department of Pediatrics, UCLA, Los Angeles, CA 90095, USA*
[f]*Department of Psychology, Emory University, Atlanta, GA 30322, USA*
[g]*Center for Interdisciplinary Brain Sciences Research, Department of Psychiatry and Behavioral Sciences, Stanford University School of Medicine, 401 Quarry Road, Stanford, CA 94305-5719, USA*

Received 15 April 2006; revised 1 June 2006; accepted 6 June 2006
Available online 9 August 2006

Applying a recently developed method to analyze gyrification with excellent spatial resolution across thousands of points across the lateral and medial cortical surface, we mapped differences in cortical surface anatomy between subjects with Williams syndrome (WS; $n=42$) and an age-matched sample of healthy subjects ($n=40$). WS subjects showed increased gyrification bilaterally in occipital regions and over the cuneus. Differences were more pronounced in the left hemisphere than in the right, with additional regions of increased gyrification in WS in the left precuneus, posterior and anterior cingulate, paracentral and mesial frontal lobe. No cortical area was significantly more convoluted in healthy subjects relative to the WS subjects. On the lateral surfaces, the direction and pattern of gyrification asymmetries were similar in WS subjects and controls; posterior brain regions had greater gyrification in the left hemisphere, while anterior brain regions showed greater gyrification in the right hemisphere. On the medial surfaces, control subjects and WS individuals differed considerably with respect to the degree but also direction of gyrification asymmetry. Our findings confirm and extend previous studies measuring cortical complexity at the global whole-brain or hemispheric levels. The observed gyrification abnormalities in individuals with WS might be related to dysfunctions in neuronal circuits and consequently contribute to the distinct cognitive and behavioral profile accompanying the disorder.

Keywords: Asymmetry; Cortex; Curvature; Lateralization; MRI

Introduction

Williams syndrome (WS) is a rare genetically determined disorder with an estimated incidence of 1 in 20–30,000 births. Affected individuals usually show mild to moderate mental retardation accompanying profound impairments in visual–motor abilities and spatial cognition (with a preferential attention to detail and relatively spared skills in face recognition). Persons with WS also demonstrate relative strengths in language (rich in vocabulary and affective prosody, but with delayed onset of grammar and vocabulary acquisition) and possess a distinct auditory sensitivity, such as attraction to music, displeasure towards certain sounds, and relatively well preserved auditory rote memory abilities. WS individuals exhibit general and anticipatory anxieties, specific phobias, as well as several attentional characteristics that can manifest as concentration problems but also as unusual looking patterns (e.g. longer, more frequent and intense looks) in social interactions. People with WS have been described as having an appetitive social drive. For a review of cognition and behavior in WS, please refer to Bellugi et al. (2001) and Mervis and Klein-Tasman (2000).

Over the past two decades numerous research groups have attempted to elucidate the neuronal correlates underlying the enigmatic behavioral and cognitive profiles associated with WS. Histological examinations show differences in neuronal cell size, coarseness, and packing density as well as neuronal organization, clustering and orientation in WS (Galaburda et al., 1994, 2002; Galaburda and Bellugi, 2000; Holinger et al., 2005). Gross anatomical analyses indicate that alterations in brain morphology also are present in WS. These morphological abnormalities involve the cerebellum, corpus callosum, amygdala, hippocampus, brain stem and cortical thickness, as well as global and regional gray and

* Corresponding author. Fax: +1 650 724 4761.
E-mail address: reiss@stanford.edu (A.L. Reiss).
Available online on ScienceDirect (www.sciencedirect.com).

1053-8119/$ - see front matter © 2006 Elsevier Inc. All rights reserved.
doi:10.1016/j.neuroimage.2006.06.018

white matter volumes and density (Jernigan and Bellugi, 1990; Wang et al., 1992; Jernigan et al., 1993; Galaburda et al., 1994, 2002; Galaburda and Bellugi, 2000; Reiss et al., 2000, 2004; Schmitt et al., 2001a,b,c; Meyer-Lindenberg et al., 2004, 2005; Thompson et al., 2005; Eckert et al., 2005). Peculiarities in the geometry (or folding pattern) of the cortical surface, such as increased global cortical complexities and regional gyrification, as well as reduced distances from the cerebral hull to the fundi of particular sulci (sulcal depths), or shortened extents of major sulci have also been detected in individuals with WS (Galaburda and Bellugi, 2000; Galaburda et al., 2001; Schmitt et al., 2002; Thompson et al., 2005; Kippenhan et al., 2005).

Although empirical data indicate major deviations in cortical surface anatomy, local effects are difficult to capture using global measures, such as fractal dimension (Thompson et al., 1996a,b, 2005). Older measures, such as the gyrification index (Zilles et al., 1988; Schmitt et al., 2002), may require some level of manual tracing – which is time-consuming and susceptible to rater bias – and the resulting measures depend on the brain's orientation (i.e. slicing direction). Finally, region-of-interest (ROI) analyses provide maximal regional specificity but make it hard to identify changes in regions that do not neatly fall within specific region boundaries determined in advance. Moreover, the analysis of a priori defined regions is compromised by inter-individual or inter-hemispheric variations in architectonic areas that may not be predictable from visible gross anatomic landmarks (Rademacher et al., 1993).

To circumvent the limitations of previous studies, we applied a recently developed method, which generates detailed and regionally specific estimates of surface gyrification at every point across the cortex, to a large sample of WS subjects and age-matched controls (N= 82). As demonstrated recently (Luders et al., 2006), our gyrification measure resembles the 3D extension of the well-known gyrification index (GI) proposed by Zilles et al. (1988), without introducing any bias from the rater or slice orientation. Given that the traditional GI revealed the degree of cortical folding to be invariant after the age of 2 years (Armstrong et al., 1995), alterations in gyrification observed with the current approach suggest neurodevelopmental effects. Using our gyrification measure, we generated maps of disease-related effects on cortical surface anatomy in an automated fashion. In addition, we generated maps indexing hemispheric differences in gyrification (hereafter referred to as gyrification asymmetry). Given the unusual profile of cognitive strengths and weaknesses in WS as well as prior evidence of differential hemispheric effects in this condition (Hickok et al., 1995; Reiss et al., 2000, 2004; Galaburda et al., 2002; Schmitt et al., 2002; Mobbs et al., 2004; Thompson et al., 2005; Kippenhan et al., 2005; Holinger et al., 2005), we used this measure to assess for potential disease-related disturbances in gyrification asymmetry.

Materials and methods

Subjects

We analyzed the brain scans of 42 subjects with genetically-confirmed Williams syndrome (mean age: 29.2±9.0 years, age range: 12–50 years; 19 M/23 F) and 40 age-matched healthy controls (age: 27.5±7.4 years; age range: 18–49 years; 16 M/24 F). This same cohort was also described in Reiss et al. (2004) and Thompson et al. (2005). All WS participants (with no history of epilepsy or other neurological conditions) were evaluated at the Salk Institute or at Cedars-Sinai Medical Center (CSMC) as part of a program project on genetics, neuroanatomy, neurophysiology, and cognition. Healthy control subjects (with no history of major psychiatric, neurological, or cognitive impairment) were recruited at both the Salk Institute and Stanford University. Handedness was determined by writing hand. There was no difference in the frequency of left or right hand writers between the groups (chi square (2,78)=0.01, ns). Thirty-seven of the 42 WS participants wrote with their right hand compared to 32 of the 36 control participants with handedness data. Writing hand data were missing for 4 control participants. All procedures were approved by the Institutional Review Boards of all three institutions, and all participants (or parents and guardians, respectively) provided informed consent.

MRI acquisition

MR images of each participant's brain were acquired with a GE-Signa 1.5 T MRI system (General Electric, Waukesha, WI, USA) located at one of three sites, as described previously (Reiss et al., 2004): (1) University of California, San Diego, (2) Scripps Clinic, San Diego, and (3) Stanford University, Stanford. In all cases, sagittal brain images were acquired with the same three-dimensional (3D) volumetric radio frequency spoiled gradient echo (spoiled gradient-recalled acquisition in a steady state) pulse sequence using the following scan parameters: TE=5 ms; TR=24 ms; 45° flip angle; matrix size=256×192; FOV=240×240 mm; slice thickness=1.2 mm, with 124 contiguous slices. Scans were preprocessed at the UCLA Laboratory of Neuro Imaging (USA) and analyzed at the University of Jena (Germany) by image analysts blinded to all subject information, including age, gender, IQ, and diagnosis.

Preprocessing

All acquired brain scans were inspected carefully and not included if of poor quality. An exhaustive description of the selection criteria and procedure is provided in Reiss et al. (2004). All MR images were processed with a series of manual and automated procedures, as summarized in Thompson et al. (2005). Briefly, image volumes were transformed into a standard space using affine transformations and corrected for intensity inhomogeneities (Sled et al., 1998). Subsequently, each individual's cortical surface was extracted and 3-dimensionally rendered using automated software (MacDonald, 1998). That is, we created spherically-parameterized mesh models of the cortical surface using signal intensity information, where each individual mesh was continuously deformed to fit the threshold intensity value that best differentiated extra-cortical cerebrospinal fluid from underlying cortical gray matter (GM). Each resulting cortical surface was represented as a high-resolution mesh of 131.072 surface triangles spanning 65,538 surface points. Given that each individual mesh parameterizes a sphere, the surface points correspond to each other, allowing us to measure gyrification and statistically test point averages across subjects and samples, in the same manner as a voxel-wise analysis of 3D image data.

Measures of local gyrification

Local gyrification was evaluated by measuring mean curvature (do Carmo, 1976) across thousands of vertices on the lateral and

medial surfaces of each individual cortical model. Mean curvature ($T_{\text{curvature}}$) at a given point is defined as

$$T_{\text{curvature}} = \sum_{v=1}^{n_v}\left(\frac{(\bar{x}_v - \tilde{x}_v)\cdot\tilde{N}_v}{B_v}\right)^2$$

where $\tilde{x}_v$ is the centroid of the neighbors of vertex v, B_v is the average distance from the centroid of each of the neighbors, $\tilde{N}_v$ is the normal vector of vertex v, and $\cdot$ is the vector product operator (MacDonald, 1998). In other words, mean curvature can be thought of as the mean angular deviation (in degrees) from a planar surface for points on a small closed loop surrounding a vertex. Local gyrification was estimated in a three-step approach as detailed in Luders et al. (2006). Briefly, calculating the mean curvature across the cortical surface results in large positive values for local maxima (corresponding to gyri) and large negative values for local minima (corresponding to sulci). To increase the signal-to-noise ratio for the mean curvature measure at a given vertex, we averaged the curvature values within a geodesic distance of 3 mm (Step I). We then calculated the absolute value of the average mean curvature resulting in curvature values greater than or equal to zero (Step II). Finally, absolute mean curvature values were smoothed using a surface-based heat kernel smoothing filter (Chung et al., 2005) with a full width at half maximum (FWHM) of 10 mm (Step III). Fig. 1 demonstrates examples of mean curvatures as well as smoothed absolute mean curvature for representative examples of folding pattern from a WS patient and normal control brain.

Analyses of group effects on gyrification

We linearly averaged the curvature values from each vertex across subjects in order to create maps of average gyrification in WS subjects and healthy controls, followed by computing the mean difference between the two groups. Finally, statistical

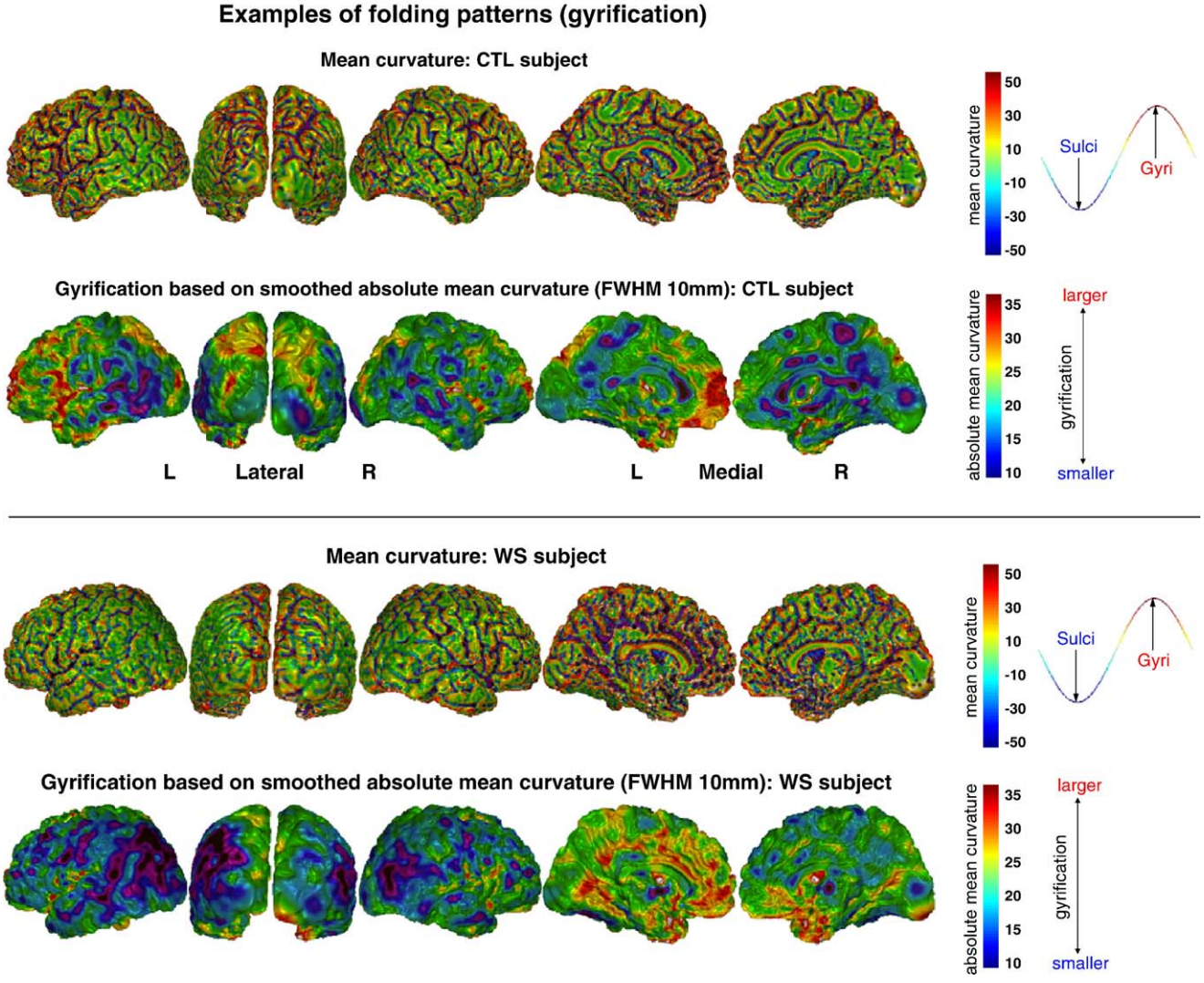

Fig. 1. Examples of folding patterns (gyrification). The two upper panels illustrate examples of folding pattern in a representative control (CTL) and WS subject. After calculating mean curvature expressed in degrees, sulci can be identified as regions with large negative values (displayed in blue), while gyri are characterized by large positive values (displayed in red). After calculating the average mean curvature within a distance of 3 mm, values are transformed into absolute values regardless of whether they represent gyri or sulci (examples not shown). Finally, surface smoothing with a heat kernel (FWHM = 10 mm) reveals higher values for areas with greater gyrification (displayed in yellow and red) and lower values for areas with smaller gyrification (displayed in blue and purple).

differences of local curvature values between WS subjects and controls were obtained using an analysis of covariance (ANCOVA) model applied to each corresponding mesh point of the cortical surface. Overall, this model permits the analysis of group differences while removing variance explained by age, gender, and total brain size[1], which were integrated as covariates into the model. We compared the groups using the resulting *t*-values and at a *p*-value threshold of 0.001. In addition, we generated color-coded maps indexing the standard deviation (SD) of mean curvature from the adjusted data (that is, where the variance explained by age, gender and total brain size was removed) for thousands of surface points across the lateral and medial cortex in participants with WS and healthy controls (Supplementary Fig. 1).

Analyses of group effects on gyrification asymmetry

To establish the presence and direction of hemispheric differences in local gyrification, we calculated lateralization indices for curvature values between corresponding vertex points using the formula (Right−Left)/0.5(Right+Left). Resulting negative values index a leftward asymmetry (that is, greater gyrification in the left hemisphere compared to the right), while positive values index a rightward asymmetry (greater gyrification in the right hemisphere compared to the left). Mean differences in hemispheric asymmetry were calculated between subjects with WS and healthy controls. Additional two-sample *t*-tests were performed to establish the significance of the asymmetry index difference between groups. Given that differences between hemispheres between samples (gyrification asymmetry differences) are usually of much lower magnitude than the sample-specific effect itself (gyrification differences), we used a lower threshold of $p<0.05$ for lateralization effects. All *p*-values were corrected for multiple comparisons using the False Discovery Rate [FDR] method (Benjamini and Hochberg, 1995).

Results

Average maps of gyrification

Fig. 2 shows the average distributions of local gyrification revealing similar patterns in controls (CTL) and WS subjects. Higher values of smoothed absolute mean curvature – indicating greater local gyrification – are seen in anterior brain regions, including the right lateral frontal cortex (in both groups), in left mesial frontal cortex (in WS) and bilaterally in the medial temporal regions (in both groups). By contrast, lower values of smoothed absolute mean curvature are found in posterior brain regions, especially in the occipital lobe, surrounding the ventral limit of the central sulcus, across the cingulate gyrus, and paracentral lobule (in both groups and both brain hemispheres).

Group differences in gyrification

As further illustrated in Fig. 2, relative to healthy controls, WS subjects exhibited increased gyrification bilaterally in occipital regions extending anteriorly over the cuneus (and precuneus in the left hemisphere), bilateral in the posterior and anterior cingulate, paracentral lobe, as well as left orbital and mesial pre-frontal cortex. Maps of mean differences between the two groups hint at areas of relatively increased gyrification in healthy controls in frontal and anterior temporal regions, as well as close to midline, near the central sulcus (all of them more pronounced in the left hemisphere), but these effects did not reach statistical significance. That is, no cortical area was significantly more convoluted in healthy subjects than subjects with WS (maps not shown).

Asymmetries in average gyrification

Fig. 3 shows the average distributions of local gyrification asymmetry revealing a similar pattern in WS subjects and controls across the lateral cortex. Leftward asymmetry – indexing a greater gyrification in the left hemisphere compared to the right – was observed in posterior brain regions (most pronounced in the occipital lobe). By contrast, rightward asymmetry was found in extended regions of the frontal lobe and inferior/posterior temporal lobe. Interestingly, different asymmetry patterns were seen – across the medial surfaces – between WS subjects and controls. Large regions of rightward asymmetry in healthy controls (illustrated in red; e.g. the precuneus), correspond to areas of leftward asymmetry in WS subjects (illustrated in blue).

WS effects on gyrification asymmetry

As shown in Fig. 3, there were significant group differences in asymmetry patterns. Across the whole lateral and medial surface, WS subjects showed numerous small clusters of stronger leftward asymmetry or diminished rightward asymmetry. These regions correspond to clusters of significantly stronger rightward asymmetry or diminished leftward asymmetry in healthy controls. Importantly, although mean differences also appear to indicate stronger rightward asymmetries in WS subjects relative to controls, those effects did not reach statistical significance (maps not shown).

Discussion

In this study, we applied a recently developed method (Luders et al., 2006) to measure the regional degree of gyrification in a well-matched sample of WS individuals versus healthy controls. We established the presence of both disease-related effects and hemispheric asymmetries. We revealed greater gyrification in WS compared to control subjects, bilaterally in occipital regions as well as across the medial cortex (Fig. 2). No cortical area was significantly more convoluted in healthy subjects compared to subjects with WS. With respect to gyrification asymmetry, WS subjects showed small but numerous clusters of stronger leftward asymmetry or diminished rightward asymmetry, across the entire medial cortical surface (Fig. 3).

Correspondence with previous findings

Our observation of increased gyrification in the occipital cortex in WS subjects, agrees with work by Galaburda et al. (1994, 2002) that found increased cell size, decreased cell packing density, and abnormal neuronal organization patterns in area 17. Others report diminished callosal areas in segments that predominantly connect parietal and occipital areas (Galaburda and Bellugi, 2000; Schmitt et al., 2001b). Further agreements between our current findings and

[1] Brain size was approximated by extracting and inverting the scaling parameters from the determinant of the affine transformation matrix generated through the prior normalization procedure.

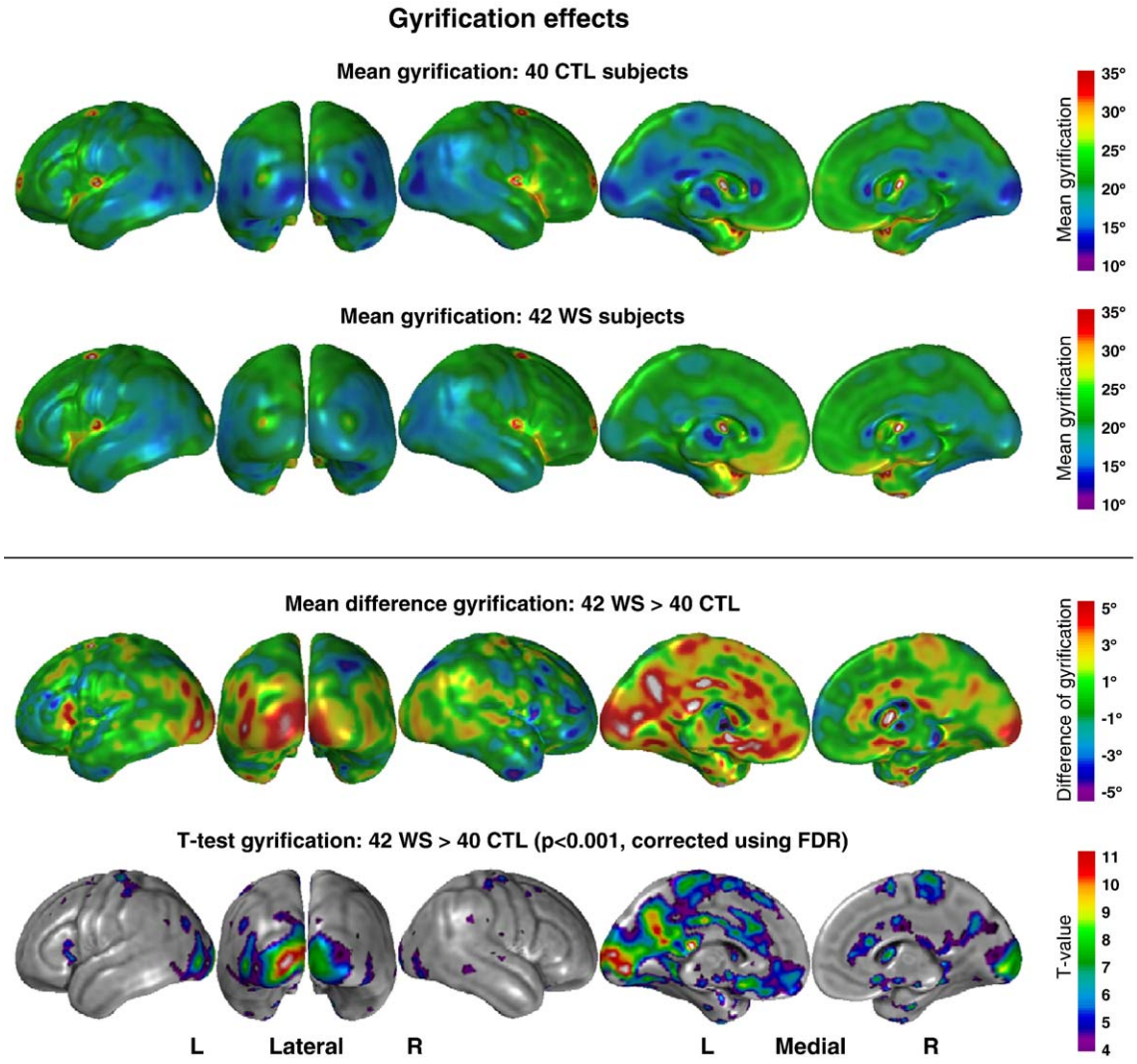

Fig. 2. Gyrification effects. The two upper panels reveal the average distribution of local gyrification in healthy controls (CTL) and subjects with WS. Curvature values are expressed in degrees, with blue and purple colors indicating regions of lower gyrification, while yellow and red indicate areas of higher gyrification. The third panel demonstrates the mean differences between subjects with WS and healthy controls. Areas with higher gyrification in WS appear in yellow and red, whereas blue and purple indicate higher gyrification in control subjects. The last panel illustrates regions of significantly increased gyrification in WS compared to normal controls (threshold $p<0.001$, corrected for multiple comparisons using FDR).

the spatial location of previous observations with respect to surface complexity and gray matter are discussed below.

Surface complexity

Our findings corroborate other recently published results demonstrating increased gyrification in WS subjects (Galaburda and Bellugi, 2000; Schmitt et al., 2002; Thompson et al., 2005). Moreover, the present study not only confirms prior global hemispheric effects in the same sample of subjects (Thompson et al., 2005), but also indicates the exact region of altered surface geometry (e.g., left and right occipital cortex and cuneus, left precuneus, posterior/anterior cingulate, paracentral lobe, orbital/mesial pre-frontal cortex). As well as improved regional specificity, the current approach can also discriminate between lateral and medial effects, which has not been possible with classical measurements of fractal dimension (Thompson et al., 2005) or gyrification index (Schmitt et al., 2002). Interestingly, this measure demonstrates that occipital cortices and medial surfaces (rather than lateral regions) show the greatest gyrification differences between WS and control subjects. By contrast, a previous study revealed reduced sulcal depths in WS in occipital and orbito-frontal regions (Kippenhan et al., 2005), but differences in the chosen measures may account for these spatial discrepancies, given that our absolute mean curvature approach measures cortical convolutions based on both gyral and sulcal characteristics (e.g. sulcal depth and length, frequency of folding). Alternatively, cohort differences may account for contrasting results. Disease-related effects may differ in samples of typically lower-functioning WS individuals (as in this study) relative to exceptional WS subjects with normal intelligence [as in Kippenhan et al. (2005)]. On the other hand, this finding might also support the hypothesis that greater amounts of cortex are buckled upward into gyri at loci where sulcal depth is observed to be reduced. This theory clearly requires further research, however.

Utilizing sulcal depth as the primary metric, Van Essen et al. (2006) compared cortical folding in 16 individuals with WS to

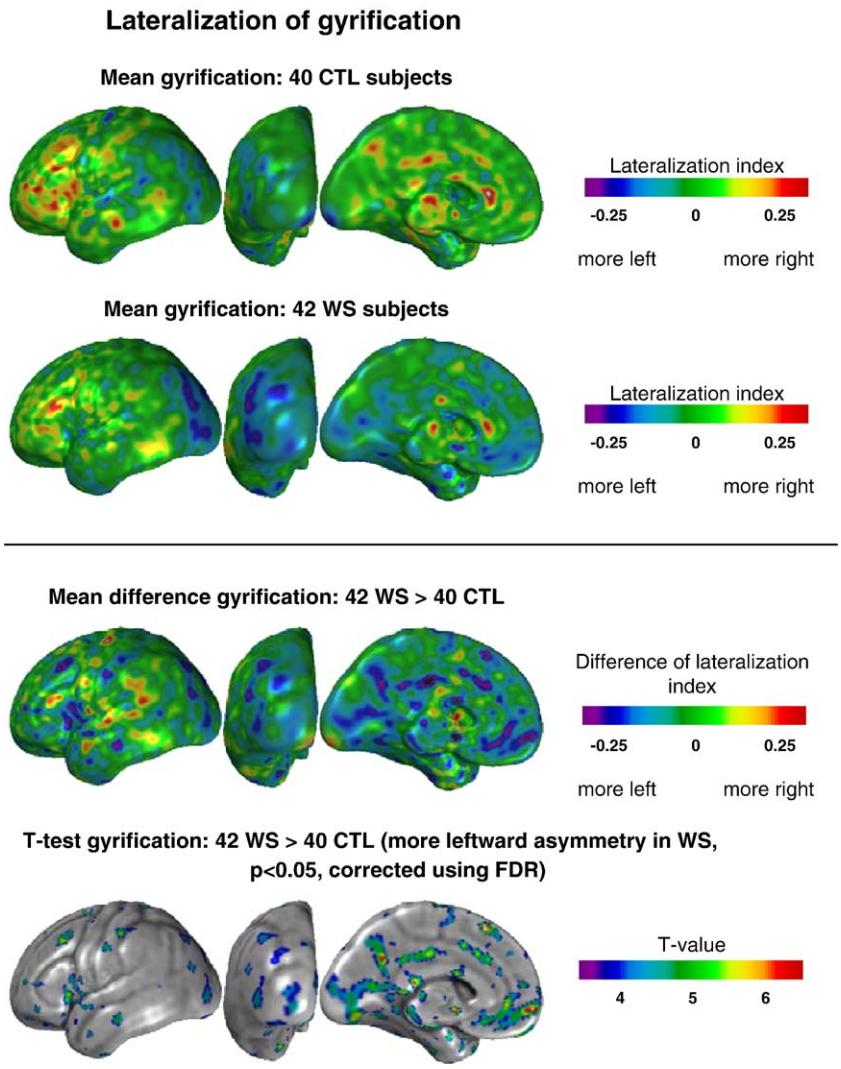

Fig. 3. Lateralization of gyrification. The two upper panels reveal the average profiles of gyrification asymmetry in healthy controls (CTL) and subjects with WS. Leftward asymmetries can be identified in regions with large negative values (displayed in blue and purple), while rightward asymmetries are characterized by large positive values (displayed in light yellow and red). The third panel reveals cortical regions where subjects with WS have stronger leftward or diminished rightward asymmetries (displayed in blue and purple) and stronger rightward or diminished leftward asymmetries (displayed in yellow and red) relative to healthy controls. Regions with increased leftward (diminished rightward) asymmetry in WS subjects correspond to regions of increased rightward (diminished leftward) asymmetry in healthy controls, and vice versa. The fourth row illustrates areas with significantly increased leftward or diminished rightward asymmetry in subjects with WS (threshold $p < 0.05$, corrected for multiple comparisons using FDR). Increased rightward and/or diminished leftward asymmetry in subjects with WS did not pass the threshold of significance (maps not shown).

healthy controls. Sulcal depths differ between the two groups across large segments of the cortex—including dorso-posterior and ventro-anterior regions of each hemisphere. Although the number of cortical locations identified as having between-group sulcal depth differences was more broadly and laterally distributed than the cortical complexity differences found in the present study, regions of the occipital, orbito-frontal and cingulate cortices were singled out in both studies. Different results between the two studies are likely due to significant methodological variation.

Gray matter volume

The spatial correspondence of clusters indicates diminished GM volume and reduced sulcal depths in WS subjects, and GM and sulcal geometry may be related (Kippenhan et al., 2005), albeit this relationship lacked consistency across cortical structures (Meyer-Lindenberg et al., 2004; Kippenhan et al., 2005). Another study detected increased GM in the anterior cingulate and orbital/mesial prefrontal cortices in WS (Reiss et al., 2004). These GM increases may relate to our present findings of increased gyrification in similar regions, supporting the assumption of a positive relationship between regional gyrification and GM volume. Other studies, however, (Reiss et al., 2000, 2004; Meyer-Lindenberg et al., 2004) reported diminished GM in parietal-occipital regions, where we detected significantly enhanced gyrification. Moreover, when correlating cortical thickness and a global measure of complexity in the same sample presented here, Thompson et al. (2005) revealed a positive correlation in healthy controls in some regions of the right hemisphere (but not left hemisphere), and neither hemisphere in WS subjects. WS

subjects had greater overall cortical complexity, but also less GM and thinner cortices, except in perisylvian regions, where the cortex was thicker than in controls. There may be no simple relationship between surface geometry (e.g., gyrification measures) and regional amounts of tissue (e.g., GM volume and cortical thickness); the presence and direction of this relationship may depend on the spatial location on the cortical surface and the population of interest (see below).

Neurodevelopmental implications

A specific neurodevelopmental mechanism associated with WS is likely to give rise to identifiable morphological abnormalities in WS subjects. For example, haploinsufficiency for one or more genes in the WS critical region of 7q is thought to contribute to early abnormalities in cortical development (Hoogenraad et al., 2002; Danoff et al., 2004; Zhao et al., 2005). Aberrant cortical development could lead to an abnormal confluence of cortex in (and prominence of) the orbito-frontal region (Reiss et al., 2004) accompanied by increased gyrification as a greater volume is folded to fit into a smaller space. The unusual shape and smaller brain volume in WS subjects, as well as their dorsal–ventral dissociations for neuroanatomy and cognition support this premise (Atkinson et al., 1997, 2003; Bellugi et al., 1999; Galaburda et al., 2001; Reiss et al., 2004; Kippenhan et al., 2005). In addition, increased gyrification may reflect differences in connectivity as it has been suggested that white matter anchors areas of connected cortex and folding occurs in relation to or surrounding these anchors (Van Essen, 1997). Finally it is also possible that aberrant gyrification patterns in WS are a secondary consequence of an (genetically determined) abnormal amount or loss of tissue, where, for example, a disproportioned loss of white matter, might lead to more gyrification. Alternatively, increased gyrification might be caused by less GM and/or a thinner cortex. That is, in order to fit more GM into the same surface the cortex has to be more gyrified (Toro and Burnod, 2005). For instance, frontal cortex, which is thicker than occipital cortex, is also less gyrified and the gyri are wider and fewer.

Functional implications

Circumscribed structural alterations in regions of the occipital and mesial prefrontal cortex, as well as the anterior cingulate are candidate anatomic substrates for some of the most prominent cognitive and behavioral characteristics in WS individuals. Our observation of relatively increased gyrification in occipital regions as well as in the cuneus and precuneus in WS may relate to visuo-spatial deficits in this population (Morris and Mervis, 2000). Extending speculations by Galaburda et al. (2002) who proposed a primary involvement of the peripheral visual cortex (on the medial surface of the occipital lobe), we also detected anomalies in cortical regions likely to represent central vision (occipital pole). Consequently, WS subjects may have structural deficits not only in visual pathways that encode information about spatial relationships and the visual control of action (Atkinson et al., 1997), but also in primary visual areas. Together with supporting observations of WS-specific gross-anatomical, cellular, and functional pecularities in occipital and parietal cortices (Galaburda and Bellugi, 2000; Reiss et al., 2000, 2004; Galaburda et al., 2002; Schmitt et al., 2002; Mobbs et al., 2004; Meyer-Lindenberg et al., 2004; Kippenhan et al., 2005; Eckert et al., 2005) aberrant caudal brain regions may be one relevant neuroanatomical substrate for visuo-spatial impairments in WS.

Similarly, attentional deficits, hyperactivity, and concentration problems as often reported in individuals with WS (Morris and Mervis, 2000) might be associated with increased cortical folding in the cingulate, as well as orbital and mesial prefrontal regions, disrupting the well-described executive attention network (Max et al., 2005). Finally, the abnormal profile of excessive social behavior in WS subjects (Morris and Mervis, 2000) may be associated with the observed structural abnormalities in the left orbito-frontal, mesial prefrontal, as well as left anterior and posterior cingulate cortices. Those structures are implicated in the processing of emotions and control of social behavior (Adolphs, 2003) and have been previously suggested as potentially contributing to disturbances in this domain of function in WS (Schmitt et al., 2002; Reiss et al., 2004; Mobbs et al., 2004; Kippenhan et al., 2005). These observations may generate new hypotheses that will lead to a more complete elucidation of links among gene, brain and cognition in WS.

Potential confounds

A potential confound for increased gyrification in WS subjects might be the group-specific brain sizes in our sample, with significantly smaller total cerebral volumes and total gray matter in WS subjects compared to healthy controls, as detailed elsewhere (Thompson et al., 2005). Notwithstanding, since total brain volume (TBV) is inextricably correlated with diagnosis, we did not statistically control for TBV because this would incorrectly eliminate some disease-specific effects. We previously noted increased gyrification in smaller female brains compared to larger male brains (Luders et al., 2004). These findings support the hypothesis that smaller overall brain volumes are associated with increased folding complexities (Galaburda et al., 2002; Luders et al., 2006). The brain volume deficit in WS is predominantly accounted for by smaller posterior regions (Galaburda and Bellugi, 2000; Reiss et al., 2000; Holinger et al., 2005). Given the increased occipital gyrification observed here, lobar volume and cortical folding may be inversely related. It is not yet clear whether the abnormal folding in WS is a secondary consequence of aberrant local shape, or directly genetically determined. Moreover, since behavior itself is capable of modifying the brain structures that support it (Galaburda and Bellugi, 2000; Draganski et al., 2004), increased gyrification is not only likely to alter functional outcomes but also prone to be modified by certain WS-specific behaviors.

Gyrification asymmetry

WS subjects and healthy controls showed a leftward asymmetry in posterior brain regions (most pronounced in the occipital lobe) and rightward asymmetry in the frontal and inferior/posterior temporal lobe. Significant asymmetry differences were detected across the lateral and medial cortical surface, where WS subjects showed small but numerous clusters of stronger leftward asymmetry and/or diminished rightward asymmetry. Although it seems to be premature to relate our hemispheric differences to any functional or behavioral outcomes, together with previous observations of abnormal asymmetry patterns in WS (Galaburda and Bellugi, 2000; Reiss et al., 2000; Holinger et al., 2005), the present asymmetry findings might serve as reference data to

stimulate further research on functional lateralization in WS. For example, event-related potential (ERP) techniques have documented that WS subjects show neither the expected left hemispheric dominance for grammatical function (Bellugi et al., 1999; Mills et al., 2001), nor right hemisphere asymmetries for face processing (Mills et al., 2000).

Acknowledgments

This work was funded by the National Institutes of Health (K02 MH01142, R01 HD31715, P01 HD33113, and U54 RR021813). Additional support was provided by research grants (R01 LM05639, P01 EB001955) and resource grants from the National Center for Research Resources (P41 RR013642 and M01 RR000865). Algorithm development for this study was partly funded by the NIA, NIBIB, the National Library of Medicine, and the National Center for Research Resources (grants AG016570, EB01651, LM05639, RR019771 to P.T.).

Appendix A. Supplementary data

Supplementary data associated with this article can be found, in the online version, at doi:10.1016/j.neuroimage.2006.06.018.

References

Adolphs, R., 2003. Cognitive neuroscience of human social behaviour. Nat. Rev., Neurosci. 4, 165–178.

Armstrong, E., Schleicher, A., Omran, H., Curtis, M., Zilles, K., 1995. The ontogeny of human gyrification. Cereb. Cortex 5, 56–63.

Atkinson, J., King, J., Braddick, O., Nokes, L., Anker, S., Braddick, F., 1997. A specific deficit of dorsal stream function in Williams' syndrome. NeuroReport 8, 1919–1922.

Atkinson, J., Braddick, O., Anker, S., Curran, W., Andrew, R., Wattam-Bell, J., Braddick, F., 2003. Neurobiological models of visuospatial cognition in children with Williams syndrome: measures of dorsal-stream and frontal function. Dev. Neuropsychol. 23, 139–172.

Bellugi, U., Lichtenberger, L., Mills, D., Galaburda, A., Korenberg, J.R., 1999. Bridging cognition, the brain and molecular genetics: evidence from Williams syndrome. Trends Neurosci. 22, 197–207.

Bellugi, U., Lichtenberger, L., Jones, W., Lai, Z., St. George, M., 2001. The neurocognitive characterization of Williams syndrome: a complex pattern of strengths and weaknesses. In: Bellugi, U., St. George, M. (Eds.), Journey from Cognition to Brain to Gene: New Perspectives from Williams Syndrome. MIT Press, Cambridge, MA.

Benjamini, Y., Hochberg, Y., 1995. Controlling the false discovery rate: a practical and powerful approach to multiple testing. J. R. Stat. Soc. B 57, 289–300.

Chung, M.K., Robbins, S.M., Dalton, K.M., Davidson, R.J., Alexander, A. L., Evans, A.C., 2005. Cortical thickness analysis in autism with heat kernel smoothing. NeuroImage 25, 1256–1265.

Danoff, S.K., Taylor, H.E., Blackshaw, S., Desiderio, S., 2004. TFII-I, a candidate gene for Williams syndrome cognitive profile: parallels between regional expression in mouse brain and human phenotype. Neuroscience 123, 931–938.

do Carmo, M.P., 1976. Differential Geometry of Curves and Surfaces. Englewood Cliffs, Prentice Hall, NJ.

Draganski, B., Gaser, C., Busch, V., Schuierer, G., Bogdahn, U., May, A., 2004. Neuroplasticity: changes in grey matter induced by training. Nature 427, 311–312.

Eckert, M.A., Hu, D., Eliez, S., Bellugi, U., Galaburda, A., Korenberg, J., Mills, D., Reiss, A.L., 2005. Evidence for superior parietal impairment in Williams syndrome. Neurology 64, 152–153.

Galaburda, A.M., Bellugi, U., 2000. V. Multi-level analysis of cortical neuroanatomy in Williams syndrome. J. Cogn. Neurosci. 12 (Suppl. 1), 74–88.

Galaburda, A.M., Wang, P.P., Bellugi, U., Rossen, M., 1994. Cytoarchitectonic anomalies in a genetically based disorder: Williams syndrome. NeuroReport 5, 753–757.

Galaburda, A.M., Schmitt, J.E., Atlas, S.W., Eliez, S., Bellugi, U., Reiss, A. L., 2001. Dorsal forebrain anomaly in Williams syndrome. Arch. Neurol. 58, 1865–1869.

Galaburda, A.M., Holinger, D.P., Bellugi, U., Sherman, G.F., 2002. Williams syndrome: neuronal size and neuronal-packing density in primary visual cortex. Arch. Neurol. 59, 1461–1467.

Hickok, G., Bellugi, U., Jones, W., 1995. Asymmetrical ability. Science 270, 219–220.

Holinger, D.P., Bellugi, U., Mills, D.L., Korenberg, J.R., Reiss, A.L., Sherman, G.F., Galaburda, A.M., 2005. Relative sparing of primary auditory cortex in Williams syndrome. Brain Res. 1037, 35–42.

Hoogenraad, C.C., Koekkoek, B., Akhmanova, A., Krugers, H., Dortland, B., Miedema, M., van, A.A., Kistler, W.M., Jaegle, M., Koutsourakis, M., Van, C.N., Verhoye, M., van der, L.A., Kaverina, I., Grosveld, F., De Zeeuw, C.I., Galjart, N., 2002. Targeted mutation of Cyln2 in the Williams syndrome critical region links CLIP-115 haploinsufficiency to neurodevelopmental abnormalities in mice. Nat. Genet. 32, 116–127.

Jernigan, T.L., Bellugi, U., 1990. Anomalous brain morphology on magnetic resonance images in Williams syndrome and Down syndrome. Arch. Neurol. 47, 529–533.

Jernigan, T.L., Bellugi, U., Sowell, E., Doherty, S., Hesselink, J.R., 1993. Cerebral morphologic distinctions between Williams and Down syndromes. Arch. Neurol. 50, 186–191.

Kippenhan, J.S., Olsen, R.K., Mervis, C.B., Morris, C.A., Kohn, P., Meyer-Lindenberg, A., Berman, K.F., 2005. Genetic contributions to human gyrification: sulcal morphometry in Williams syndrome. J. Neurosci. 25, 7840–7846.

Luders, E., Narr, K.L., Thompson, P.M., Rex, D.E., Jancke, L., Steinmetz, H., Toga, A.W., 2004. Gender differences in cortical complexity. Nat. Neurosci. 7, 799–800.

Luders, E., Thompson, P.M., Narr, K.L., Toga, A.W., Jancke, L., Gaser, C., 2006. A curvature-based approach to estimate local gyrification on the cortical surface. NeuroImage 29, 1224–1230.

MacDonald, D., 1998. A method for identifying geometrically simple surfaces from three dimensional images. PhD thesis, McGill University.

Max, J.E., Manes, F.F., Robertson, B.A., Mathews, K., Fox, P.T., Lancaster, J., 2005. Prefrontal and executive attention network lesions and the development of attention-deficit/hyperactivity symptomatology. J. Am. Acad. Child Adolesc. Psych. 44, 443–450.

Mervis, C.B., Klein-Tasman, B.P., 2000. Williams syndrome: cognition, personality, and adaptive behavior. Ment. Retard. Dev. Disabil. Res. Rev. 6, 148–158.

Meyer-Lindenberg, A., Kohn, P., Mervis, C.B., Kippenhan, J.S., Olsen, R. K., Morris, C.A., Berman, K.F., 2004. Neural basis of genetically determined visuospatial construction deficit in Williams syndrome. Neuron 43, 623–631.

Meyer-Lindenberg, A., Kohn, P.D., Kolachana, B., Kippenhan, S., Inerney-Leo, A., Nussbaum, R., Weinberger, D.R., Berman, K.F., 2005. Midbrain dopamine and prefrontal function in humans: interaction and modulation by COMT genotype. Nat. Neurosci. 8, 594–596.

Mills, D.L., Alvarez, T.D., St, G.M., Appelbaum, L.G., Bellugi, U., Neville, H., 2000. III. Electrophysiological studies of face processing in Williams syndrome. J. Cogn. Neurosci. 12 (Suppl. 1), 47–64.

Mills, D.L., Alvarez, T.D., St. George, M., Appelbaum, L.G., Bellugi, U., Neville, H., 2001. Neurophysiological markers of face processing in Williams syndrome. In: Bellugi, U., St. George, M. (Eds.), Journey from Cognition to Brain to Gene: Perspectives from Williams Syndrome. MIT Press, Cambridge, MA.

Mobbs, D., Garrett, A.S., Menon, V., Rose, F.E., Bellugi, U., Reiss, A.L., 2004. Anomalous brain activation during face and gaze processing in Williams syndrome. Neurology 62, 2070–2076.

Morris, C.A., Mervis, C.B., 2000. Williams syndrome and related disorders. Annu. Rev. Genomics Hum. Genet. 1, 461–484.

Rademacher, J., Caviness Jr., V.S., Steinmetz, H., Galaburda, A.M., 1993. Topographical variation of the human primary cortices: implications for neuroimaging, brain mapping, and neurobiology. Cereb. Cortex 3, 313–329.

Reiss, A.L., Eliez, S., Schmitt, J.E., Straus, E., Lai, Z., Jones, W., Bellugi, U., 2000. IV. Neuroanatomy of Williams syndrome: a high-resolution MRI study. J. Cogn. Neurosci. 12 (Suppl. 1), 65–73.

Reiss, A.L., Eckert, M.A., Rose, F.E., Karchemskiy, A., Kesler, S., Chang, M., Reynolds, M.F., Kwon, H., Galaburda, A., 2004. An experiment of nature: brain anatomy parallels cognition and behavior in Williams syndrome. J. Neurosci. 24, 5009–5015.

Schmitt, J.E., Eliez, S., Bellugi, U., Reiss, A.L., 2001a. Analysis of cerebral shape in Williams syndrome. Arch. Neurol. 58, 283–287.

Schmitt, J.E., Eliez, S., Warsofsky, I.S., Bellugi, U., Reiss, A.L., 2001b. Corpus callosum morphology of Williams syndrome: relation to genetics and behavior. Dev. Med. Child Neurol. 43, 155–159.

Schmitt, J.E., Eliez, S., Warsofsky, I.S., Bellugi, U., Reiss, A.L., 2001c. Enlarged cerebellar vermis in Williams syndrome. J. Psychiatr. Res. 35, 225–229.

Schmitt, J.E., Watts, K., Eliez, S., Bellugi, U., Galaburda, A.M., Reiss, A.L., 2002. Increased gyrification in Williams syndrome: evidence using 3D MRI methods. Dev. Med. Child Neurol. 44, 292–295.

Sled, J.G., Zijdenbos, A.P., Evans, A.C., 1998. A nonparametric method for automatic correction of intensity nonuniformity in MRI data. IEEE Trans. Med. Imag. 17, 87–97.

Thompson, P.M., Schwartz, C., Lin, R.T., Khan, A.A., Toga, A.W., 1996a. Three-dimensional statistical analysis of sulcal variability in the human brain. J. Neurosci. 16, 4261–4274.

Thompson, P.M., Schwartz, C., Toga, A.W., 1996b. High-resolution random mesh algorithms for creating a probabilistic 3D surface atlas of the human brain. NeuroImage 3, 19–34.

Thompson, P.M., Lee, A.D., Dutton, R.A., Geaga, J.A., Hayashi, K.M., Eckert, M.A., Bellugi, U., Galaburda, A.M., Korenberg, J.R., Mills, D.L., Toga, A.W., Reiss, A.L., 2005. Abnormal cortical complexity and thickness profiles mapped in Williams syndrome. J. Neurosci. 25, 4146–4158.

Toro, R., Burnod, Y., 2005. A morphogenetic model for the development of cortical convolutions. Cereb. Cortex. 15, 1900–1913.

Van Essen, D.C., 1997. A tension-based theory of morphogenesis and compact wiring in the central nervous system. Nature 385, 313–318.

Van Essen, D.C., Dierker, D., Snyder, A.Z., Raichle, M.E., Reiss, A.L., Korenberg, J., 2006. Symmetry of cortical folding abnormalities in Williams syndrome revealed by surface-based analyses. J. Neurosci. 26, 5470–5483.

Wang, P.P., Hesselink, J.R., Jernigan, T.L., Doherty, S., Bellugi, U., 1992. Specific neurobehavioral profile of Williams' syndrome is associated with neocerebellar hemispheric preservation. Neurology 42, 1999–2002.

Zhao, C., Aviles, C., Abel, R.A., Almli, C.R., McQuillen, P., Pleasure, S.J., 2005. Hippocampal and visuospatial learning defects in mice with a deletion of frizzled 9, a gene in the Williams syndrome deletion interval. Development 132, 2917–2927.

Zilles, K., Armstrong, E., Schleicher, A., Kretschmann, H.J., 1988. The human pattern of gyrification in the cerebral cortex. Anat. Embryol. (Berl) 179, 173–179.